INNSPUB

Journal of Biodiversity and Environmental Sciences (JBES)
ISSN: 2220-6663 (Print) 2222-3045 (Online)
Vol. 9, No. 1, p. 185-193, 2016
http://www.innspub.net

RESEARCH PAPER OPEN ACCESS

Magnetic field interpretation using singular value decomposition method based on correlation coefficient of eigenimages

Ata Eshaghzadeh*, Roghayeh Alsadat Kalantari

Graduate student of geophysics, Institute of Geophysics, University of Tehran, Iran

Article published on July 21, 2016

Key words: Correlation coefficient, Eigenimage, magnetic, Singular Value Decomposition (SVD).

Abstract

Magnetic investigations can yield important information about geological structures. Singular Value Decomposition (SVD) is a very powerful tool for analysis of the geophysical data set chiefly potential fields. In this paper, a new technique for demonstration of near-subsurface features with short wavelength using magnetic eigenvectors and eigenimage is proposed which separate the residual anomalies from magnetic map background (total magnetic field). Also, is exhibited a new method based on correlation coefficient between eigenimages for threshold determination. Using the SVD, a matrix of magnetic data set can be decomposed to a series of eigenimages. Finally, the SVD method eventuate two layers of singular value images that the layer reconstructed of threshold value to last eigenimages show local magnetic anomalies. The results obtained from the synthetic data set, with and without random noise, have been discussed. The method is demonstrated on real magnetic data set surveyed from Iran. The results show the good performance of the proposed method.

***Corresponding Author:** Ata Eshaghzadeh ✉ eshaghzadeh.ata@gmail.com

Introduction

Magnetic data observed in geophysical surveys are the sum of magnetic fields produced by all underground sources. The targets for specific surveys are often small-scale structures buried at shallow depths, and the magnetic responses of these targets are embedded in a regional field that arises from magnetic sources that are usually larger or deeper than the targets or are located farther away. As a matter of fact the total magnetic field is the aggregate the rigional and residual magnetic fields. Correct estimation and removal of the regional field from the initial field observations yields the residual field produced by the target sources (Li *et al*., 1998). Land or airborn surveying of the magnetic field of the Earth and preparation of the maps of the magnetic field variations are used universal as part of exploration programs for mineral or hydrocarbon resources. Interpretation of magnetic data is very ambiguous. Qualitative and quantitative analysis are carried out on the residual field data, and the depend ability of the interpretation depends to a great extent upon the accurate and exact separation of the regional and residual fields. Few papers have presented specifically methods in this issue. Most of the work is concerned with gravity data, but many of the methods can be extended to magnetic data processing, e.g., least square approach (Agocs, 1951; Oldham and Sutherland, 1955; Skeels, 1967) and using digital filters (e.g., Zurflueh, 1967; Gupta and Ramani, 1980; Pawlowski and Hansen, 1990; Pawlowski, 1994).

In linear algebra, the singular value decomposition (SVD) is a decomposer instrument of a $m \times n$ real or complex matrix to a $m \times m$ real or complex unitary matrix, a $m \times n$ rectangular diagonal matrix with nonnegative real numbers on the diagonal and a $n \times n$ real or complex unitary matrix. The SVD method has many useful applications in signal processing, statistics, geophysics etc. The SVD as a signal processing tool has been used in geophysical data processing, e.g., for compressing seismic reflection profiles (Jackson *et al*., 1991), ground-penetrating radar processing (Cagnoli and Ulrych, 2001), enhancing weak signals in vertical seismic profiles (Freire and Ulrych, 1988). Fedi *et al*. (2005) used of the SVD to study the regularizing properties of the Tikhonov problem. Li (2005) used the multi-fractal SVD for feature extraction and anomaly identification for mineral exploration. The SVD can be used for signal and noise separation (Glifford, 2005; Vrabie *et al*., 2004). Ulrych *et al*. (1988) illustrated the application of SVD to seismic profiles. Shib and Dimri (2013) used of SVD to interpretation of gravity data. Wang *et al*. (2012) employed of the multifractal singular value decomposition for delineating geophysical anomalies associated with molybdenum occurrences in the Luanchuanore field (China). Eshaghzadeh and Salehyan (2015) have applyied SVD method for regional and residual anomalies separation from gravity field.

In this paper, is proposed a new technique based on the singular value decomposition of the magnetic data set for segregation the residual magnetic field from the total magnetic field whiles the residual field map exhibit the more detail of the magnetic anomaly sources. In this study, the total magnetic data is analysed by means of extracting information from the eigenimages with the help of singular value decomposition (SVD) and correlation criteria. The method is checked for artificial and real magnetic data from Iran. The results have been compared with the polynomial fitting technique.

Methodology

The magnetic anomaly results from the contrast in magnetization when rocks with different magnetic properties are adjacent to each other (W. Lowrie 2007). Two main corrections are applyed for magnetic measurements. First, elimination of the short-term variations, inclusive the diurnal (or daily) variation and magnetic storms and another is subtraction the main geomagnetic field from magnetic measurements. The difference between the observed and expected values extracted of the International Geomagnetic Reference Field (IGRF) is a magnetic anomaly. In many of magnetic case studies,

before reduction to the pole (RTP) of the obtained magnetic anomaly, it is needed the magnetic effect of the regional anomaly to be eliminated. However, after correction of magnetic field data set, the signals of the regional field background and noise remain in the local magnetic anomaly map. Severance the local anomaly from the regional field background can be a efficient aid for the magnetic field interpretation. The Singular Value Decomposition (SVD) is a useful tool to achieve this separation.

The equation for singular value decomposition of matrix $W_{m\times n}$ is the following:

$$W = SUV^T \qquad (1)$$

Where S is an m × n left eigenvector matrix, U is an n × n diagonal matrix. The elements of $U_{n\times n}$ are only nonzero on the diagonal, and are called the singular values. V^T is also an n × n right eigenvector matrix and T stands for transpose. The singular values of matrix $W_{m\times n}$ are the positive entries of $U_{n\times n}$ which are distributed in decreasing order along its main diagonal and are equal to positive square roots of the eigenvalues (λ_i) of the covariance matrices W^TW & WW^T . If W is m rows by n columns, it must be initially converted to a 1-D vector form [the size is (m × n) × 1]. The covariance matrices can be calculated as the following equation

$$\mathrm{cov}(W) = E\left[(W - E[W])(X - E[W])^T\right] \quad (2)$$

Where E is expected value.
moreover,
$U=\mathrm{diag}(u_1,u_2,\ldots,u_r)$
Where r=rank (W), $u_1 \geq u_2 \geq \ldots \geq u_r$, $u_i = \sqrt{\lambda_i}$.

By convention, the ordering of the singular vectors is determined by high-to-low sorting of singular values, with the highest singular value in the upper left index of the matrix $U_{n\times n}$. Note that for a square, symmetric matrix $W_{m\times n}$, singular value decomposition is equivalent to diagonalization, or solution of the eigenvalue problem.

The singular value decomposition of matrix $W_{m\times n}$ can be also written as follows:

$$W = \sum_{i=1}^{r} s_i u_i v_i^T \quad (3)$$

Where r is the rank of matrix $W_{m\times n}$, u_i is the i-th eigenvector of covariance matrix WW^T,v_i is the i-th eigenvector of covariance matrix W^TW, s_i is the i-th singular value of matrix $W_{m\times n}$, and $u_i v_i^T$ is an m×n matrix of unitary rank called the i-th eigenimage of matrix $W_{m\times n}$ (e.g. the first eigenimage, $s_1 u_1 v_1^T$).

According to Eq. (2), the original matrix can be rebuilt with all of the eigenimages. Also, if some specific eigenimags are selected, a sub-matrix can be reconstructed. Eigenvectors that correspond to big eigenvalues are the directions in which the data have large variance. The eigenvector corresponding to the highest eigenvalue retains the most significant amount of information. The second eigenvector corresponds to the second highest eigenvalue retains information of second significance, similarly and so on to the smallest eigenvalue. We exploit of this SVD property for separation the regional fields background and residual fields from magnetic anomaly map.

The regional-field background usually has smoother variations than those of the local anomalies. The regional magnetic field background can presume as the major variability of the data set and can be approximated by the first eigenimags. The local magnetic anomaly is delineated with short wavelength and can be derived by the latest eigenimages. The SVD method is used directly on the magnetic data M to reveal local (residual) magnetic anomaly. Thus matrix data set M is decomposed as

$$M = M_{rfb} + M_{loc} = \sum_{i=1}^{k} s_i u_i v_i^T + \sum_{j=k+1}^{n} s_j u_j v_j^T \quad (4)$$

Where k is defined as threshold. The first k eigenimages of data matrix represent the regional

fields background map M_{rfb} and the attained eigenimages of the *k+1* to rank *n* exhibit the local anomaly map M_{loc}.

Threshold determination

The correlation coefficient between two numerical series *x* and *y* (*correl(x,y)*) is computed according to:

$$correl(x,y)=\frac{\mathrm{cov}(x,y)}{\sigma_x\sigma_y}=\frac{\sum_{i=1}^{n}(x-\bar{x})(y-\bar{y})}{\sqrt{\sum_{i=1}^{n}(x-\bar{x})^2\sum_{i=1}^{n}(y-\bar{y})^2}} \quad (5)$$

Where σ_x and σ_y are standard deviation of the numerical series *x* and *y* respectively. $\bar{x}$ and $\bar{y}$ are the average of two numerical sets *x* and *y* with *n* elements.

In the first step is reconstructed the magnetic field image using the first eigenimage (m_1), latter using two first eigenimages, namely the 1st and 2nd eigenimages (m_2), third reconstructed image using the 1st to 3rd eigenimages (m_3) and so on and so forth. Therefore according to the rank of the magnetic data matrix, can be created the magnetic field map (m_1, m_2, m_3, ... , m_{rank}). In the next step, the correlation between m_i and m_{i+1} (where i=1, 2, 3, ..., rank) is computed according to eq. (5). Whenever the estimated correlation coefficient between two magnetic field map, that is, m_i and m_{i+1}, was equal to 1, *i* is considered as threshold.

Rectangular prism model

The equation for the total field magnetic anomaly at any point P (x, y, 0) due to a vertical prism whose sides are parallel to the coordinate axes (Fig. 1) is given by (Rao and Babu 1991)

$$\Delta T(x,y,0)=G_1\ln F_1+G_2\ln F_2+G_3\ln F_3+G_4F_4+G_5F_5 \quad (6)$$

Where

$$G_1=EI(Mr+Nq),G_2=EI(Lr+Np),G_3=EI(Lq+Mp),$$
$$G_4=EI(Nr-Mq),G_5=EI(Nr+Lp),$$

Where EI is the intensity of magnetization, L, M, N, are the direction cosines of magnetization, and p, q, r are the direction cosines of the geomagnetic field.

Also,

$$F_1=\frac{(R_2+\alpha_1)(R_3+\alpha_2)(R_5+\alpha_1)(R_8+\alpha_2)}{(R_1+\alpha_1)(R_4+\alpha_2)(R_6+\alpha_1)(R_7+\alpha_2)}$$

$$F_2=\frac{(R_2+\beta_1)(R_3+\beta_1)(R_5+\beta_2)(R_8+\beta_2)}{(R_1+\beta_1)(R_4+\beta_1)(R_6+\beta_2)(R_7+\beta_2)}$$

$$F_3=\frac{(R_2+h_2)(R_3+h_1)(R_5+h_1)(R_8+h_2)}{(R_1+h_1)(R_4+h_2)(R_6+h_2)(R_7+h_1)}$$

$$F_4=\arctan\frac{\alpha_2h_2}{R_8\beta_2}-\arctan\frac{\alpha_2h_1}{R_6\beta_2}-\arctan\frac{\alpha_2h_2}{R_4\beta_1}+\arctan\frac{\alpha_1h_2}{R_2\beta_1}-\arctan\frac{\alpha_2h_1}{R_7\beta_2}$$
$$+\arctan\frac{\alpha_1h_1}{R_5\beta_2}+\arctan\frac{\alpha_2h_1}{R_3\beta_1}-\arctan\frac{\alpha_1h_1}{R_1\beta_1}$$

$$F_5=\arctan\frac{\beta_2h_2}{R_8\alpha_2}-\arctan\frac{\beta_2h_2}{R_6\alpha_1}-\arctan\frac{\beta_1h_2}{R_4\alpha_2}+\arctan\frac{\beta_1h_2}{R_2\alpha_1}-\arctan\frac{\beta_2h_1}{R_7\alpha_2}$$
$$+\arctan\frac{\beta_2h_1}{R_5\alpha_1}+\arctan\frac{\beta_1h_1}{R_3\alpha_2}-\arctan\frac{\beta_1h_1}{R_1\alpha_1}$$

and

$$R_1=\sqrt{\alpha_1^2+\beta_1^2+h_1^2},$$
$$R_2=\sqrt{\alpha_1^2+\beta_1^2+h_2^2},$$
$$R_3=\sqrt{\alpha_2^2+\beta_1^2+h_1^2},$$
$$R_4=\sqrt{\alpha_2^2+\beta_1^2+h_2^2},$$
$$R_5=\sqrt{\alpha_2^2+\beta_2^2+h_1^2},$$
$$R_6=\sqrt{\alpha_1^2+\beta_2^2+h_2^2},$$
$$R_7=\sqrt{\alpha_2^2+\beta_2^2+h_1^2},$$
$$R_8=\sqrt{\alpha_2^2+\beta_2^2+h_2^2},$$
$$\alpha_1=a_1-x',\alpha_2=a_2-x',$$
$$\beta_1=b_1-y',\beta_2=b_2-y',$$

If the horizontal sides of the prism are not parallel to the coordinate axes, but are rotated by an angle o with respect to the geographic north (Fig. 1). then we have to choose a new coordinate system (x‘, y‘) parallel to the horizontal sides of the rectangular prism. The point o on the observation plane remains the origin of the new (x‘, y‘) as well as old (x, y) coordinate systems. Then the (x, y) coordinates to be replaced by the new coordinates (x‘, y‘) given by (Rao and Babu 1991)

$$x'=x\cos\theta+y\sin\theta$$
$$y'=-x\sin\theta+y\cos\theta$$

If I and D are the inclination and declination of the geomagnetic field, the direction cosines of the field vector are given by

$$p=\cos I\cos(D-\theta)$$
$$q=\cos I\sin(D-\theta)$$
$$r=\sin I$$

If I_o, and D_o, are the inclination and declination of the magnetization vector, then its direction cosines are given by

$$L = \cos I_0 \cos(D_0 - \theta)$$
$$M = \cos I_0 \sin(D_0 - \theta)$$
$$N = \sin I_0$$

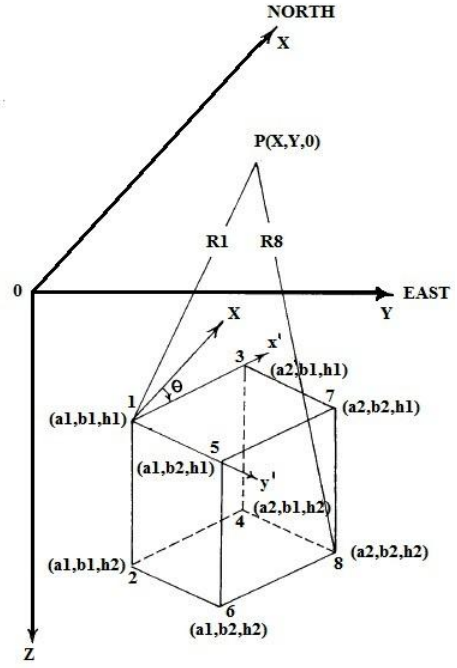

Fig. 1. Three-dimensional rectangular prism.

Synthetic example

The SVD method is tested to the synthetic magnetic dataset generated as a response of 3D rectangular prism models underneath earth surface to evaluate its effectiveness.

We have generated a model composed of three prisms located at different depths into 500 m × 500 m grid size (Fig. 2a). Fig. 2b displays the magnetic field of the synthetic model which prisms have the same magnetization intensity (5 A/m).

The supposed declination and inclination angles for the magnetization are 45 and zero degrees, respectively (horizontal magnetization). For the geomagnetic field the declination and inclination angles have been assumed zero and 90 degrees, respectively (reduced to pole).

The size of the large rectangular body as the regional anomaly source is 350 m × 340 m × 170 m at 30 m depth. In this model, there are two separate prisms as local anomalies : upper, size is 150 m × 50 m × 10 m at 5 m depth in the western-eastern (left to right) direction and lower, size is 50 m × 100 m × 10 m at 10 m depth in the north-south direction.

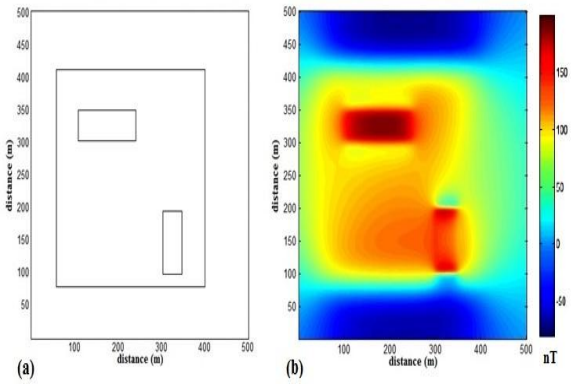

Fig. 2. a) The location of the rectangular prisms in 500 m × 500 m grid. b) The total magnetic field of the shown model in (a).

For this model, the correlation coefficient between m_1 and m_2 0.9904 and between m_2 and m_3 1 was gained. So, the threshold *k* is considered as 2 in eq. (4). Fig.3 display the analysis results of the magnetic data shown in Fig. 2b using SVD method. Fig.3a and b have been reconstructed using the two first eigenimages and remaining eigenimages, respectively. In Fig.3b, the effect of the regional magnetic field background (Fig. 3a) has been eliminated and the residual anomalies have been detected with high precision.

For investigation the sensitivity of the SVD method to disorder, normally distributed random noise with a mean 50 and standard deviation 2 added to the magnetic data in Fig. 2b. Fig. 4 show the synthetic magnetic field for the model shown in Fig. 2a which random noise added to it.

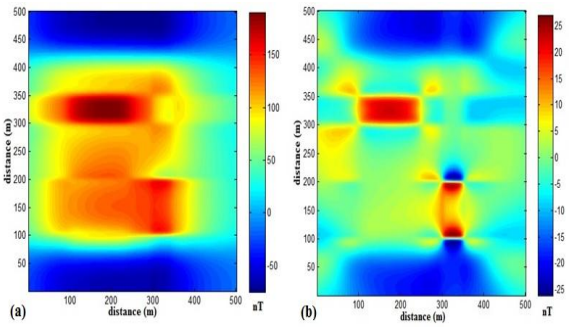

Fig. 3. a) Reconstructed image from the 1st and 2nd eigenimages. b) Reconstructed image from the 3rd to final eigenimages. This shape disply the local anomaly map.

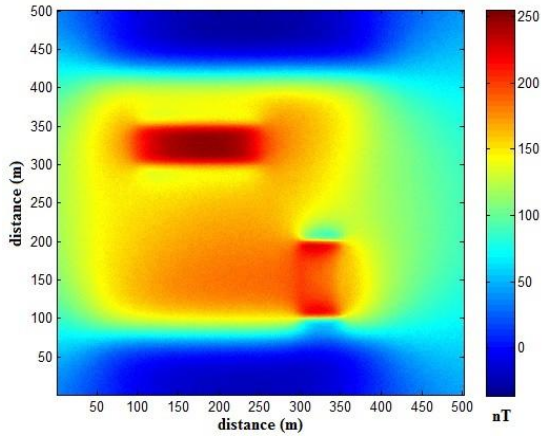

Fig. 4. The synthetic magnetic field for the model shown in Fig. 2 (a) which random noise with a mean 50 and standard deviation 2 added to it.

For synthetic model with noise, the correlation coefficient between m_1 and m_2 0.9836, between m_2 and m_3 0.9952 and between m_3 and m_4 1 was gained. So, the threshold *k* is considered as 3 in eq. (4). Fig. 5 exhibit the decomposition results of the synthetic magnetic data shown in Fig. 4 using SVD. Fig. 5a and b have been reconstructed using the three first eigenimages and remaining eigenimages, respectively. Satisfactory results have been achieved in the presence of the noise.

Field example

The under survey zone is located in the north of Kerman province, Iran, covering an area about 440 m by 230 m. Kerman province can be a part of Central Iran zone in structural units and extent of sedimentary basins viewpoint.

Paleozoic to Mesozoic geological formation of the study region consists of dolomite and dolomitic limestone,

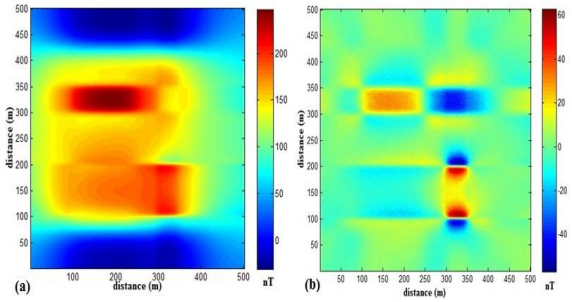

Fig. 5. a) Reconstructed image from the 1st to 3rd eigenimages. b) Reconstructed image from the to 4th to final eigenimages. this shape disply the local anomaly map.

orbitolina limestone with marl, alternations of marly biomicrite with marl, sandy micrite and siltstone. Quaternary sediments include sand dunes and sheets, silt and clay. Percambrian outcrops comprise volcanic rock, quartzite, sandstone and shale. The main iron ores in this area are from the oxide group consisting of hematite and magnetite. The aim of the magnetic field measurments is metal resources discovery.

Based on the model IGRF, the geomagnetic field inclination and declination angles in this part are 46.99˚ and 2.8˚, respectively. Fig. 6 illustrate the magnetic reduction to pole data of the surveyed area. The geological structure or metal deposits with high magnetic susceptibility are located in the relatively high magnetic anomaly area.

Before decomposition and analysis the magnetic data using SVD, the threshold was estimated based on correlation coefficient of the eigenimages. The correlation coefficient between the rebuilded maps from the 1st to 3rd and 1st to 4th eigenimages is one. So, the threshold *k* is considered as 3 in eq. (4). Fig. 7 show the reconstructed regional magnetic field background using three first eigenimages.

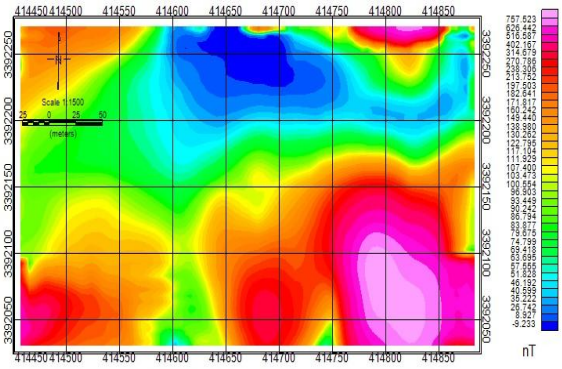

Fig. 6. Reduction to pole magnetic anomaly map.

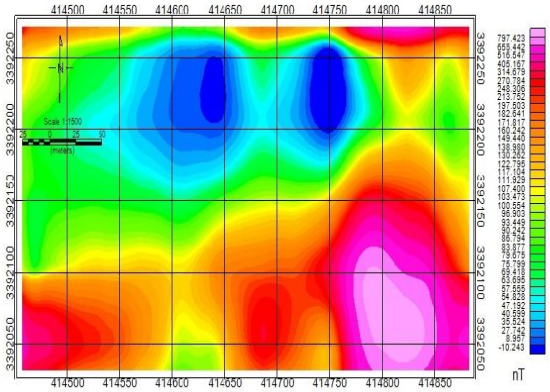

Fig. 7. Reconstructed map from the 1st to 3rd eigenimages as the regional magnetic field background.

Fig. 8. show the reconstructed residual magnetic anomalies using 4th to final eigenimages, namely 84th eigenimage which is equal to the rank value of the magnetic data matrix. Fig. 9 represent the residual field separated by the polynomial fitting method that is non smoother than the obtained residual magnetic field from SVD and include less information. The data in Fig.s 8 and 9 vary from -203.635 to 224.026 nT and -205.608 to 321.77 nT respectively.

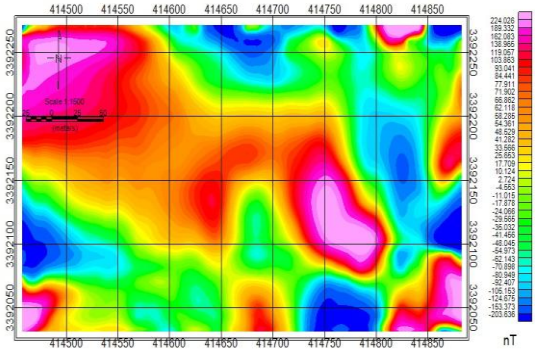

Fig. 8. Reconstructed map from the 4th to 84th eigenimages as the local magnetic anomalies.

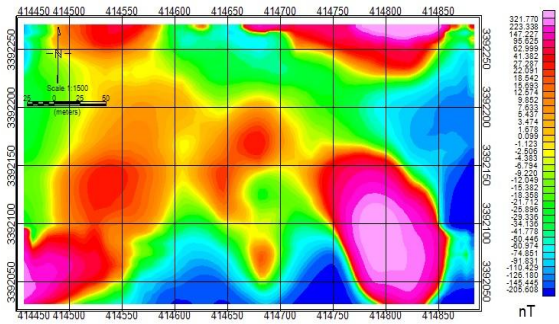

Fig. 9. The generated residual magnetic map using the polynomial fitting method.

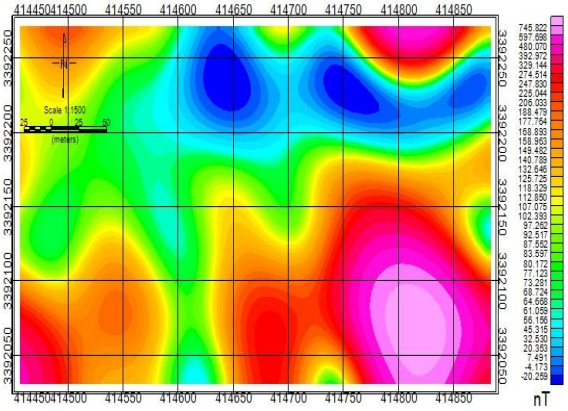

Fig.10. The result of the use the low past filter with cutoff wavelength 100 m on the reduction to pole magnetic anomaly map (Fig. 6).

Discussion

In this paper the singular value decomposition (SVD) method has been suggested for separation the residual anomalies as object and the region field as background. The utility of SVD depends on the choice the correct threshold.

In this study, has computed the correlation coefficient between the two magnetic maps generated by eigenimages. The correlation coefficient of one has determined the threshold k in the equation 4. Revelation of the anomalies with short wavelength (shallow-source) as the local field and exploratory targets helps to the more accurate interpretation of magnetic maps. Hence, various methods have been proposed for detecting and enhancing potential field data, such as analytic signal, tilt angle, theta map and so on. An important capability and distinguishing for SVD is the ability to detect weak signals in the data.

The efficiency of the SVD as a separator technique has been shown on synthetic magnetic data set with and without random noise. The proposed method has been separated the residual (local) magnetic field from the total magnetic fields shown in the Figs. 2a and 4 well and the satisfactory results have been yielded. The Figs. 3 and 5 show the consequences of the separation. In both recent Figs, the magnetic field of the smaller rectangles as the causing the residual field (Figs. 2a and 5a) has been extracted from the total magnetic field truly. The SVD method performance for noisy data is as acceptable as the without nois data. The SVD method not only indent the more detail of magnetic field due to the near surface geological structures (Fig. 8), separate the anomalies with long wavelength due to regional magnetic field (deeper-source). The SVD method has detected the regions with the high magnetic intensity very well and has obtained better results than polynomial fitting technique. Reconstructed map using three first eigenimages in Fig. 7 contain the general information of the geological structures of the survey region, that is, the regional magnetic field. Fig. 10 shows the result of the apply the low past filter with cutoff wavelength 100 m on the reduction to pole magnetic anomaly map (Fig. 6) which has the conformity to map shown in Fig. 7. The consequences of synthetic and real magnetic field analysis using eigenimages derived by means of the SVD demonstrate the acceptable efficiency of the method for feature extraction and anomaly enhancement for mineral exploration.

References

Agocs WB. 1951. Least-squares residual anomaly determination: Geophysics **16**, 686–696.

Cagnoli B, Ulrych TJ. 2001. Singular value decomposition and wavy reflections in ground penetrating radar images of base surge deposits. Journal of Applied Geophysics **48**, 175–182.

Eshaghzadeh A, Salehyan N. 2015. regional and residual anomalies separation from gravity field using singular value decomposition (SVD) method. AGU-SEG Workshop Abstracts, Keystone, Colorado, USA.

Fedi M, Hansen PC, Paoletti V. 2005. Analysis of depth resolution in potential-field inversion. Geophysics **70**, P. A1–A11.

Freire S, Ulrych T. 1988. Application of singular value decomposition to vertical seismic profiling. Geophysics **53**, 778–785.

Glifford GD. 2005. Singular value decomposition independent component analysis for blind source separation. HST582J/6.555 J/16.456 J, Biomedical signal and Image Processing.

Gupta VK, Ramani N, 1980. Some aspects of regional residual separation of gravity anomalies in a Precambrian terrain: Geophysics **45**, 1412–1426.

Jackson G, Mason I, Greenhalgh S. 1991. Principal component transforms of triaxial recordings by singular value decomposition. Geophysics **56**, 528–533.

Li QM. 2005,GIS-based multifractal/inversion methods for feature extraction and applications in anomaly identification for mineral exploration, Ph.D. thesis, York University, Toronto, Canada 211 pp.

Li Y, Oldenburg DW. 1998. Separation of regional and residual magnetic field data. Geophysics **63**, 431-439.

Lowrie W. 2007. Fundamentals of Geophysics. Cambridge University Press, New York.

Oldham CHG, Sutherland DB. 1955. Orthogonal polynomials and their use in estimating the regional effect: Geophysics **20**, 295– 306.

Pawlowski RS, Hansen RO. 1990. Gravity anomaly separation by Wiener filtering: Geophysics **55**, 539–548.

Pawlowski RS. 1994. Green's equivalent-layer concept in gravity band-pass filter design: Geophysics **59**, 69–76.

Rao DB, Babu NR. 1991. A rapid method for three-dimensional modeling of magnetic anomalies, Geophysics **56(2)**, 1729-1737.

Shib SG, Dimri VP. 2013. Interpretation of gravity data using eigenimage with Indian case study: A SVD approach, Journal of Applied Geophysics **95**, 23–35.

Skeels DC. 1967. What is residual gravity?: Geophysics **32**, 872–876.

Ulrych TJ, Freire SLM, Siston P. 1988. Eigenimage processing of seismic sections. S22—Seismic Sessions: Signal-to-noise Enhancement II: SEG Expanded Abstracts **7,** p. 1261. http://dx.doi.org/10.1190/1.1892508.

Vrabie VD, Mars JI, Lacoume JL. 2004. Modified singular value decomposition by means of independent component analysis. Signal Processing **84**, 645–652.

Wang G, Zhang S, Yan C, Xu G, Ma M, Li K, Feng Y. 2012. Application of the multifractal singular value decomposition for delineating geophysical anomalies associated with molybdenum occurrences in the Luanchuan ore field (China). Journal of Applied Geophysics **86**, 109–119.

Zhao B, Chen Y. 2011. Singular value decomposition (SVD) for extraction of gravity anomaly associated with gold mineralization in Tongshi gold field, Western Shandong Uplifted Block, Eastern China. Nonlinear Processes in Geophysics **18**, 103–109.

Zurflueh EG. 1967. Application of two-dimensional linear wavelength filtering: Geophysics **32**, 1015–1035.